MICROFACIES OF LATE PLEISTOCENE TRAVERTINE DEPOSITS IN JORDAN

Issa M. Makhlouf [1a*], Khalil M. Ibrahim[2a], Sana' M. Al-Thawabteh[3a], and Ali R. El Naqah[4b]

[a]Department of Earth and Environmental Sciences, Prince El-Hassan Bin Talal, Faculty of Natural Resources and Environment; The Hashemite University, P.O. Box 330127, Zarqa 13133, JORDAN. Email: makhlouf@hu.edu.jo[1]; ibrahim@hu.edu.jo[2]; sana.thawabteh@gmail.com[3]
[b]Department of Water Management and Environment, Prince El-Hassan Bin Talal Faculty of Natural Resources and Environment; The Hashemite University, P.O. Box 330127, Zarqa 13133, JORDAN. Email: elnaqa@hu.edu.jo[4]
*Corresponding Author: makhlouf@hu.edu.jo
Received: 18th Jan 2021 Accepted: 9th Sep 2021 Published: 30th Jun 2022
DOI: https://doi.org/10.22452/mjs.vol41no2.8

ABSTRACT The Late Pleistocene travertine outcrops from Deir Alla, Suwayma, and Az Zara were investigated, and their microfacies were identified. The microfacies of the Deir Alla travertines include micrite and spar groundmass, shrubs, crystalline crusts, a stromatolite-like structure, peloids, and cements. Shrub travertine includes spar calcite-coated stems with probably microbial micritic clumps. The crystalline crust travertine displays an alternation of micrite and sparite laminae. The micritic laminae are dark-coloured. Bundles of radial spar crystals are associated locally with micritic groundmass. The crystalline crust developed where biogenic activity is limited. Peloidal microfacies are less than 0.25 mm in diameter, cryptocrystalline, pale-dark green in colour, elliptical to spherical in shape, and usually associated with microorganisms. The microfacies of the Suwayma and Az Zara travertines include crystalline calcite rhombs and other composite scalenohedral crystals. They occur as small anhedral-subhedral crystals, monocrystalline to some polycrystalline, corroded, subrounded, and mainly coated with iron oxide and/or clay minerals. Peloids, ooids, and oncoids are common. They are dark-green coloured, cryptocrystalline to microcrystalline carbonates of spherical and ellipsoidal shape with less than 1 mm in diameter. Rich flora travertines include reed and paper-thin rafts with leaf impressions encrusted on moss cushions. The flora observed in the upper part of the Suwayma section was identified as charophyte oospores (gyrogonites). A few grains of quartz are present as small subhedral-euhedral crystals, monocrystalline, corroded, rounded, and mainly coated with iron oxide. The iron is irregularly distributed among the laminae and voids and is occasionally replaced by carbonates. The described macrophyte encrustation structures probably represent algae, cyanobacteria, or bryophytes. All samples of micrite and spar calcite appear as groundmass.

Keywords: Jordan, Dead Sea, travertine, Pleistocene, microfacies

1. INTRODUCTION

Travertines, also known as terrestrial limestone, are chemically precipitated calcite and aragonite around springs, lakes, and streams. Such deposits display rapid vertical and lateral changes due to subaerial precipitation from calcium bicarbonate-rich waters (Claes et al., 2015, 2017). Localised travertine deposits are developed in active tectonic areas, especially from deep hydrothermal waters (Pedley, 1994; Ford and Pedley, 1996; Della Porta et al., 2017a). The spring water responsible for the Late Pleistocene travertine precipitation in Jordan (Ibrahim et al., 2017) is derived from the underlying Mesozoic sandstones and rose along faults to adjacent slopes similar to those described by Guo and Riding (1998) in Italy. These low-energy, fine-grained lithofacies are commonly developed in a concentric pattern (Capezzuoli et al., 2014). Many factors are responsible for the variability of travertine facies, such as the natural setting of the spring, water level fluctuations, flow direction, organic activity, climatic changes, subaerial reworking, and paedogenic conditions (Claes et al., 2015, 2017). The rapid change of water chemistry when spring water cools and mixes with rainwater is also an important factor.

This paper aims to contribute to the knowledge of the Jordanian travertines because these deposits have not been previously described in detail and are important for the study of evaporative systems, Pleistocene palaeoenvironmental reconstructions, and geomicrobiology, among others. In particular, the Dead Sea system has a strong appeal due to its intriguing and endangered environment, which is currently experiencing super-fast lake level decreases, leading to salt dissolution and sinkhole formation at its shores. Therefore, the information on Pleistocene deposits of the Dead Sea is important to help reconstruct past environmental and tectonic history, especially on the Jordan side, where little information is available in international journals. Due to the scarce literature on these travertine occurrences in Jordan, this study was performed to present the microfacies of the travertine occurring in three sites from the east of the Jordan Valley–Dead Sea Transform: (1) Deir Alla (35° 35' 58.14", 32° 6' 43.68"); (2) Suwayma (35° 35' 31.86", 31º 44' 0.24"); and (3) Az Zara (35° 33' 41.88", 31° 36' 5.70") (Figure 2; Table 1).

The Late Pleistocene travertine that occurs along the north-eastern bank of the Jordan Valley has been deposited around the hot springs of El-Hamma on the lower course of the Yarmouk River in north Jordan and the Az Zara hot springs (Figure 1) at the north-eastern corner of the Dead Sea (Abu Ajamieh, 1980; Obeidat, 1992; Al-Thawabteh, 2006; Ibrahim et al., 2017). Abu Ajamieh (1980) studied the physical and chemical properties of some of the Az Zara springs and assigned those hypothermal springs to having temperatures higher than 34 °C.

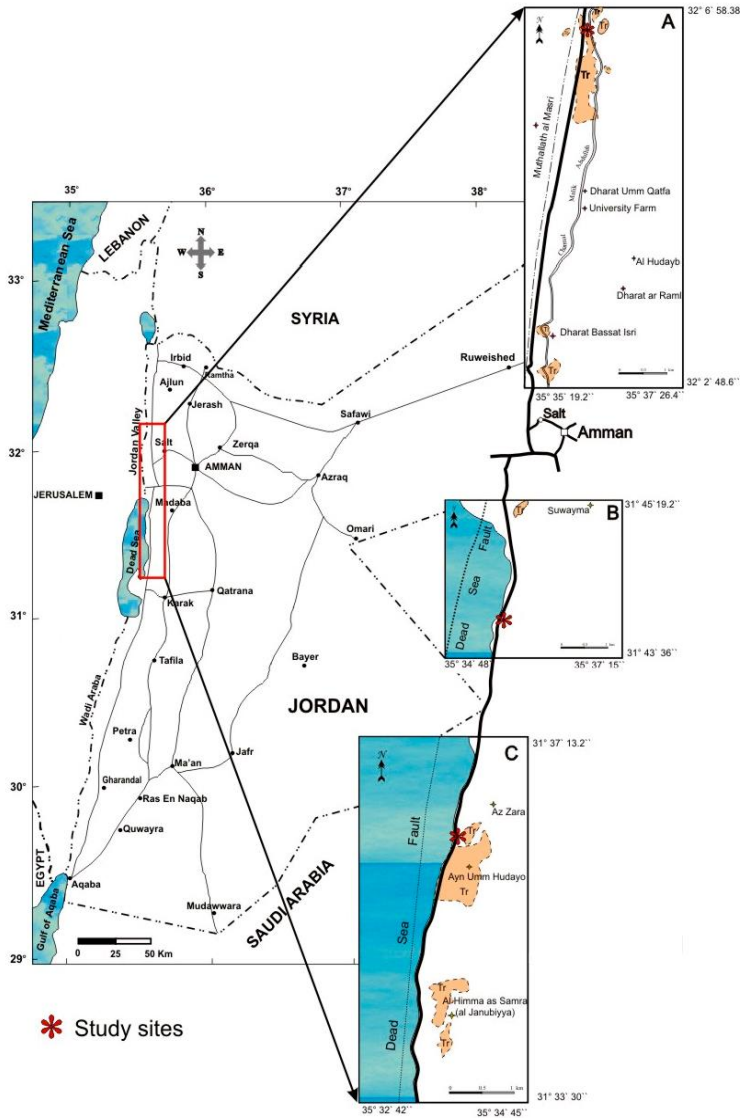

Figure 1. Location of the study areas at Deir Alla, Suwayma, and Az Zara in Jordan

2. METHODOLOGY

The Deir Alla (42-m thick), Suwayma (78-m thick), and Az Zara (46-m thick) travertine outcrops at the eastern flank of the Dead Sea–Jordan valley transform were investigated (Figure 1; Table 1). Three vertical lithological sections were measured and described (Figure 2). The outcrops are located along a nearly 90-km long transect parallel to the Jordan valley–Dead Sea from Deir Alla in northern Jordan to Az Zara in the south (Figure 1). The identification of travertine lithotypes and their vertical stacking patterns, depositional geometries, and stratigraphic architectures on the outcropping strata and adjacent saw-cut quarry face were also investigated.

Travertine precipitates in different depositional conditions and displays variations in colour, appearance, bedding, porosity, texture, and composition. Travertine encompasses different lithofacies based on field characteristics and petrographical features. Some examples of lithofacies include crystalline crusts, shrubs, reeds, pisolites, paper-thin rafts, coated gas bubbles, stromatolites, and brecciated travertine.

Stratigraphic logs were used to obtain the microfacies data, as shown in Figure 2. The microfacies were identified after studying the petrographic properties of the thin sections and scanning them with an electron microscope (SEM, FEI Quanta 600). Microscopic characteristics are the most critical features to examine in order to comprehend travertine's formation, mineralogy, and diagenesis processes. A polarising microscope was used to identify the mineralogic composition and the sequence of diagenetic events. Thirty thin sections were prepared from the collected travertine samples.

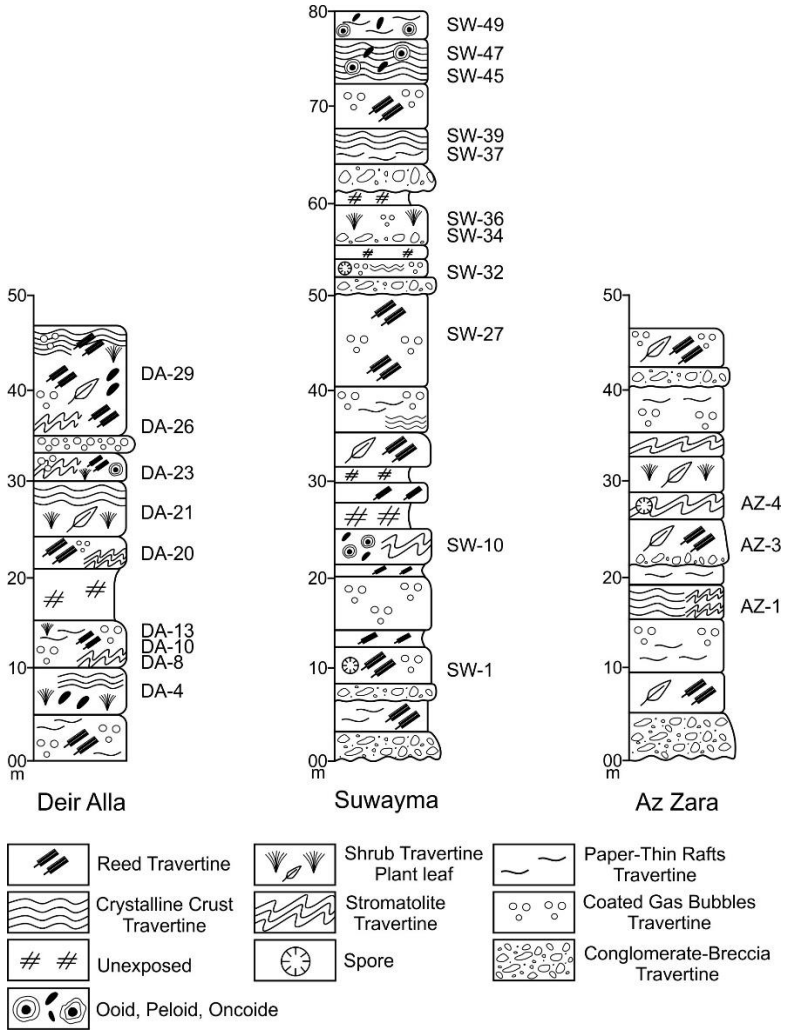

Figure 2. Stratigraphic logs of three Late Pleistocene travertine exposures along a N–S transect from Deir Alla (DA) in the Jordan Valley, Suwayma (SW), and Az Zara (AZ) to the Dead Sea, Jordan

Table 1. Description and interpretation of travertine microfacies in the studied areas

Location	Microfacies	Thin sections & SEM	Components and Diagenesis	Depositional Environment
Deir Alla	Crystalline crust	DA-4, DA-8, DA-10, DA-13, DA-29	Micrite, sparite, and columnar crystals; cementation and compaction by pressure solution.	High flow velocity of water on smooth slopes, terraced slopes, pool rims, and vertical walls.
	Shrub	DA-4, DA-8, DA-20, DA-21, DA-23, DA-26	Spar and micrite calcite; vertically dark-coloured shrub; sparmicritization cementation.	Terrace pools; shallow and low angle slope pools; warm water.
	Stromatolite	DA-8, DA-20, DA-26	Organosedimentary structure; recrystallisation.	Trapping, binding, and low precipitation; metabolic activity of algae and/or cyanophytes.
	Peloidal	DA-4, DA-26	Aggregates of peloids; clotted mesofabric.	Pond sub-environment; lake.
Suwayma	Crystalline	SW-32, SW-45, SW-27, SW-34, SW-36, SW-37, SW-39, SW-47, SW-45	Rhombic and scalenohedral calcite crystals.	High flow velocity of water on smooth slopes, terraced slopes, pool rims, and vertical walls.
	Shrub	SW-39		Terrace pools; shallow and low angle slope pools; warm water.
	Stromatolite	SW-8	Organosedimentary structure.	Trapping, binding, and low precipitation; metabolic activity of algae.
	Peloids	SW-10, SW-22, SW-47, SW-49	Alternated micrite and sparite laminae in a fan-like growth.	Shallow water saturated with calcium carbonate; warm springs.
	Ooids	SW-10	Elliptical with a clear nucleus associated with bacterial branching clumps, which occur in a radial pattern almost perpendicular to the surface.	Shallow water saturated with calcium carbonate; warm springs; high energy and agitation conditions.
	Oncoids	SW-10	Elliptical with an irregular concentric lamina developed around semi-clear nuclei.	Very shallow water with available algae.
	Spores	SW-1, SW-32	Charophyte oospores (gyrogonites) with woody tissues; cementation; recrystallisation.	Lacustrine conditions; dammed lakes; low-energy bench-type carbonate pond; terraced-like areas.
Az Zara	Crystalline	AZ-1	Rhombic and scalenohedral calcite; small subhedral-euhedral; monocrystalline; quartz crystals coated with iron oxide cementation; dolomitisation; recrystallisation.	High flow velocity of water on smooth slopes, terraced slopes, pool rims, and vertical walls; iron oxide-rich fluid circulation; cementation.
	Stromatolite	AZ-4, AZ-1	Dome and wavy stromatolite-like structure; iron oxide-rich fluid circulation.	Trapping, binding, and low precipitation and metabolic activity of algae and/or cyanophytes;
	Spores	AZ-3, AZ-4	Stems and twigs; mouldic pores infilled with calcite spar; woody tissues; cementation; recrystallisation; Charophyte oospores (gyrogonites); recrystallisation.	Fluvio-Palustrine area.
	Shrub	AZ-3	Occurring as spar calcite and microspar taking a bush-like shape.	Shallow and low angle slope.

3. RESULTS

The description of microfacies is based on field observations, numerous thin sections, and scanning electron microscopy examination of the samples. Several travertine microfacies types were distinguished based on their texture and carbonate fabric characteristics (Figure 3; Table 1).

They were labelled in this study because they have been most commonly used by Chafetz and Folk (1984), Özkul et al. (2014), and Della Porta et al. (2017a and 2017b)

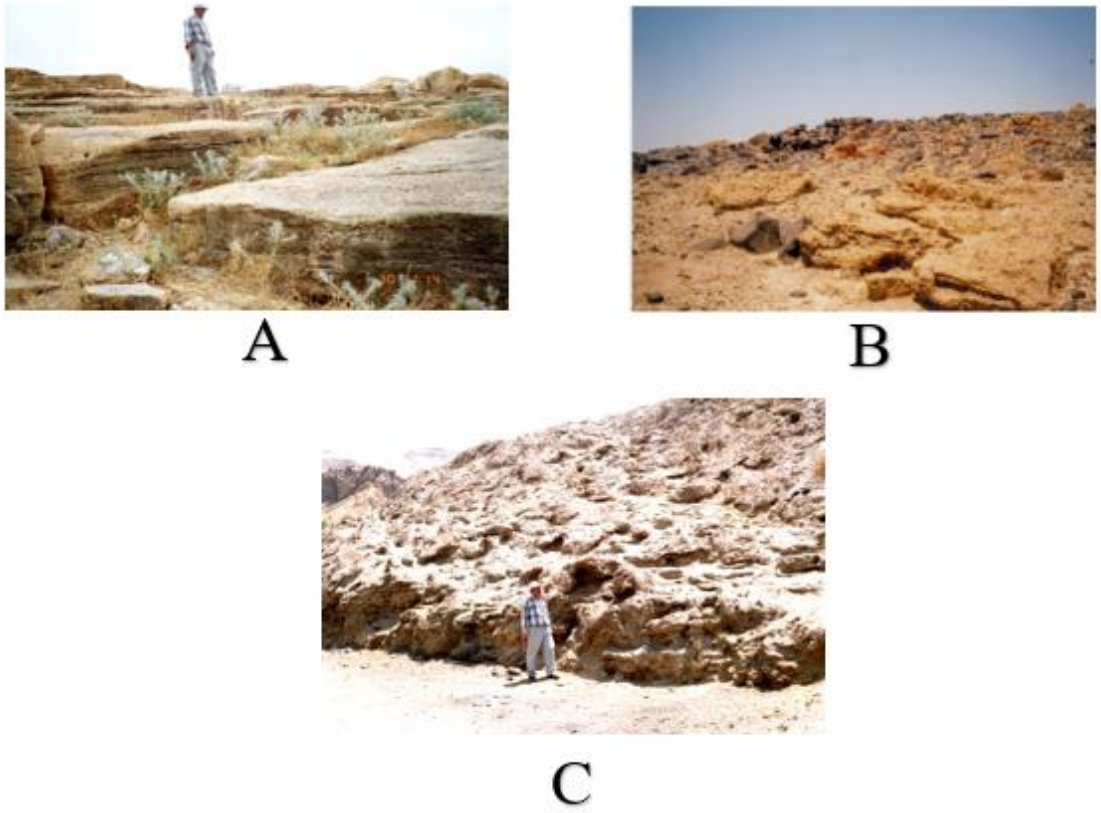

Figure 3. Field photographs: (A) the Deir Alla travertines showing different levels of thinly bedded strata; (B) the Suwayma travertines' exposure; and (C) the Az Zara travertines' exposure showing stacked travertine strata

3.1 Microfacies of the Deir Alla Travertines

3.1.1. Crystalline Crust Travertine Microfacies

The vast majority of travertine grains are composed of calcium carbonate (aragonite or calcite). Figures 4A and 4B show minute calcite rhombs mixed with larger composite crystals. Under the polarising microscope, calcite is mainly present as micrite and spar groundmass. Secondary calcite may fill pores or replace some minerals. Quartz makes up less than 3%, which is presented as small anhedral-subhedral, monocrystalline, and subrounded grains in the micritic groundmass. Most of the studied samples contain iron oxides (Figure 4C), occurring more or less as diffuse masses within the groundmass (Figures 4D and 5A; Table 1).

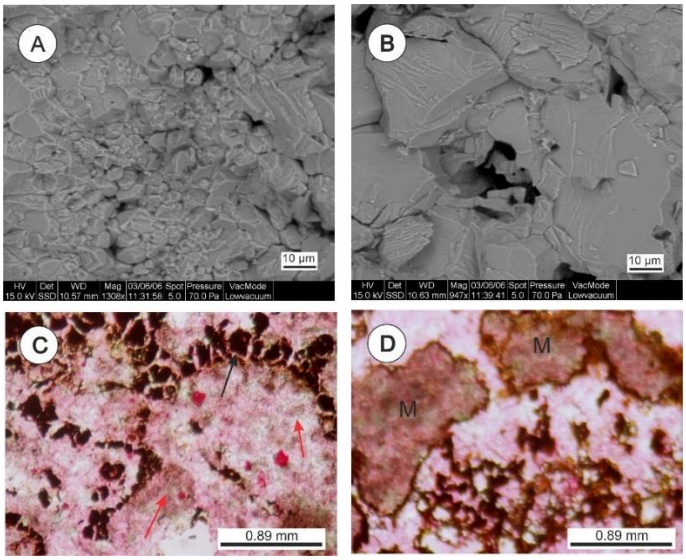

Figure 4. SEM and photomicrographs of the Deir Alla travertines (Crystalline Crust Travertine Microfacies) showing: **(A)** SEM image shows minute calcite rhombs mixed with larger composite crystals (sample № DA-8**,** Mag. 1308x); **(B)** SEM image shows larger composite calcite crystals (sample № DA-8, Mag. 947x); **(C)** photomicrograph shows round iron oxide within calcite groundmass (black arrow). Spar crystals under the micritic clumps' support resemble recrystallisation of micrite into sparite (red arrows) (sample № DA-26, stained, plane polarising light (PPL x10); **(D)** photomicrograph shows diffuse iron masses within the calcitic groundmass. The cloudy micrites (M) developed through sparmicritization on the spar crystals (sample № DA-4, stained, plane polarising light (PPL), x10)

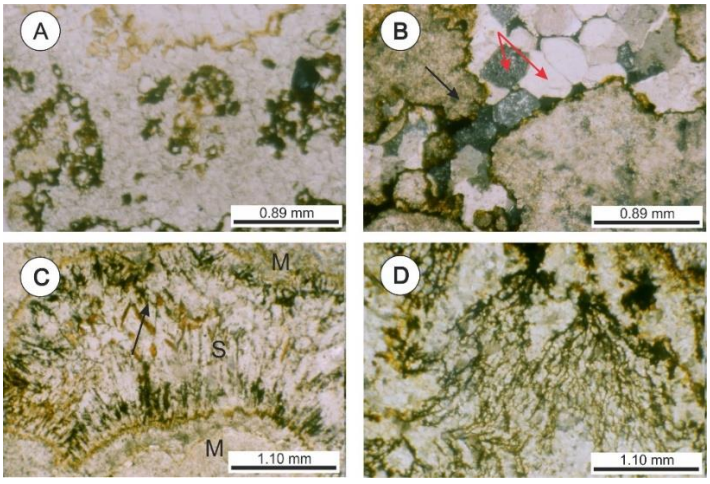

Figure 5. Photomicrographs of the Deir Alla travertines showing (Crystalline Crust Travertine Microfacies): **(A)** different types of diffuse iron masses within the microspar calcite groundmass (sample № DA-8, non-stained, plane polarising light (PPL), x10); **(B)** iron compounds coating the cavities (black arrow), cavities completely infilled with spar calcite that represents mosaic cement (red arrows) (sample № DA-29, non-stained, cross polarising light (XPL), x10); **(C)** crystalline crust as alternation of micrite (M) and sparite (S) laminae, spar calcite enriched in iron and noticed as stylolitic texture (black arrow) (sample № DA-10, non-stained, plane polarising light (PPL), x4); **(D)** dendritic structure includes iron oxides possessing through the calcitic groundmass (sample № DA-13, non-stained, cross polarising light (XPL), x4)

Iron compounds also coat cavities that, in some places, are totally or partially infilled with calcite spar (Figure 5B). Iron-rich (Fe) solutions intruded into the calcite groundmass and made a zigzag feature (Figure 5C). The stylolitic and microstylolitic structures in travertine indicate the compaction effect inserted by pressure solution (Figure 5C). Loading causes stress to be inserted at grain contacts, causing solution to form at the contacts and subsequent carbonate incorporation into the solution, which provides material for re-precipitation as cement infill of surrounding pores (Greensmith, 1978). In some places, the iron oxides intruded into the microspar calcite, forming a dendritic texture (Figure 5D).

Dolomite and high-iron dolomite (ankarite) are rare, reported mainly in the middle part of the Deir Alla section. They occur as unstained rhombic crystals. Also, the unstained spots in travertine thin sections indicate the presence of clay minerals appearing as whitish to greenish in colour (Figures 6A and 6B). The Deir Alla travertines are mainly composed of shrubs, crystalline crusts, a stromatolite-like structure, peloids, and cements (Table 1). The nature, distribution, and characteristics of each microfacies are discussed briefly below.

The crystalline crusts are composed of calcite crystals with a feather-like calcite arranged in superposed syntaxial rows of growth (Figures 7B and 7D). Generally, the crystalline crust is more common in the Deir Alla section, but little has been observed in the middle part of this section. Under the microscope, the Deir Alla crystalline crusts are seen as an alternation of micrite and sparite laminae. The micritic laminae are commonly dark-coloured.

The dark micritic laminae show the development of solution pores. The sparite laminae may contain iron oxides in variable ratios (Figure 7C). Radially grown spar crystals are common (Figures 7D, 8A) on the micritic groundmass and are organised into bundles in some places. Locally, the spar crystals have grown into columnar crystals. The term “Palisades” is used to describe spar crystals when they are present as parallel arrays (Figure 8B). Unfractured crystals and fractured pieces are common. Fractured crystals infill interspaces and micritic groundmass, similar to those described by Özkul et al. (2002) in the Denizli basin in Turkey.

3.1.2. Shrub Travertine Microfacies

The term “shrub” was introduced for travertines by Kitano (1963) and has been commonly used by Chafetz and Folk (1984), Claes et al. (2015, 2017), and many others, to describe the morphological appearance of the outer mm-to-cm scaled structures.

The shrub travertine occurs in the lower and upper parts of the Deir Alla section. Under the microscope, the shrubs are composed of spar and micrite crystal associations, which are organised into variable styles. In general, the crystal shape of both types shows no clear separating boundary between them. The Deir Alla thin sections were prepared perpendicular to the bedding plains. The spaces among the dark-coloured micritic vertically aligned shrub forms are infilled with secondary mosaic spar calcite (Figures 6C and 6D; Table 1). However, in the thin sections that are parallel or nearly oblique to the bedding plain, dark micritic clumps display a mottled texture among the sparite, which appears as dispersed patches (Figure 7A) (Özkul et al., 2002).

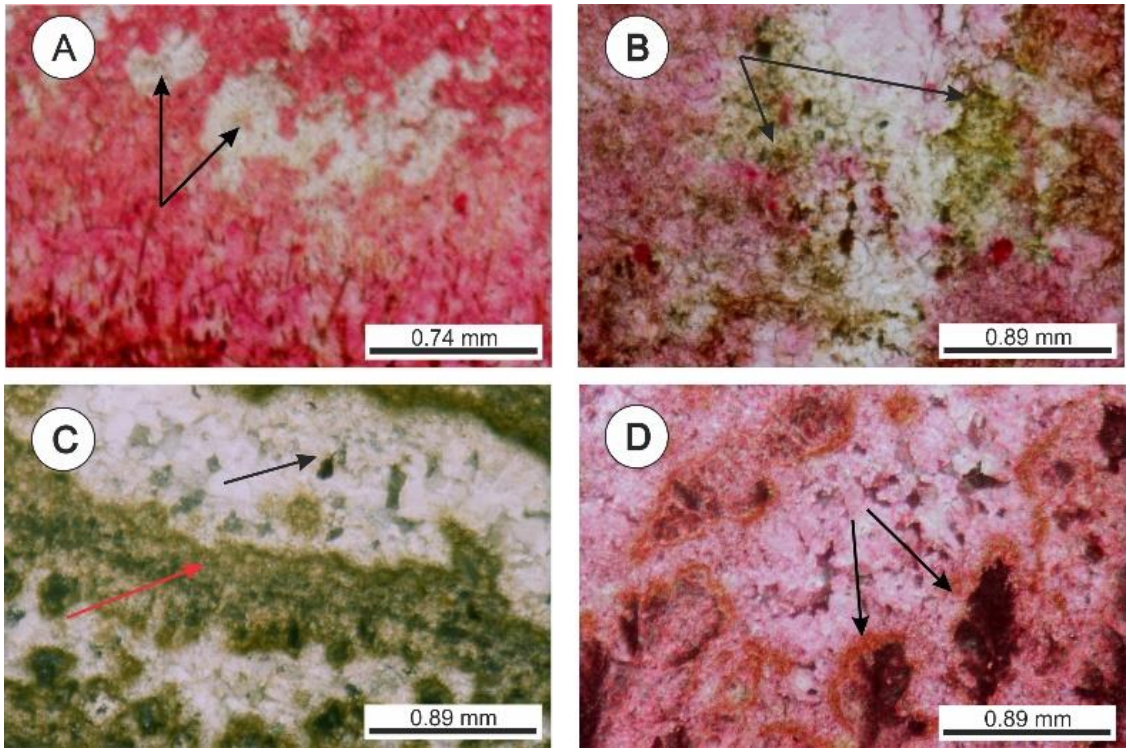

Figure 6. Photomicrographs of the Deir Alla travertines (Crystalline Crust Travertine Microfacies "A and B," and Shrub Travertine Microfacies "C and D") showing: **(A)** sample № DA-23, non-stained clay mineral patches distributed throughout the micritic calcite (black arrows) (stained, Plane polarising light (PPL), x20); **(B)** another view similar to figure (16-A) for more details (black arrows) (sample № DA-8, stained, plane polarising light (PPL), x10); **(C)** shrub travertine includes spar calcite coated stems (black arrow) within a dark green micrite matrix (red arrow) (sample № DA-26, non-stained, cross polarising light (XPL), x10); **(D)** dark-coloured micritic shrub forms that expand upward and enriched by iron oxides (sample № DA-26, stained, cross polarising light (XPL), x10)

It is obvious that the occurrence of the micritic clumps in irregular form gave rise to the mottled appearance that resembles the bubbles and pustules described by Della Porta (2015). The clumps are probably microbial in origin and were defined by Chafetz and Guidry (1999) as bacterial shrubs. Furthermore, the cloudy appearance of micrites was formed on the spar crystals (Figure 4D; Table 1). The shrub travertine is subdivided into three kinds: bacterial (Figure 7A); crystal; and ray crystal "feather calcite" (Figure 7B) (Chafetz and Guidry, 1999; Croci et al., 2016).

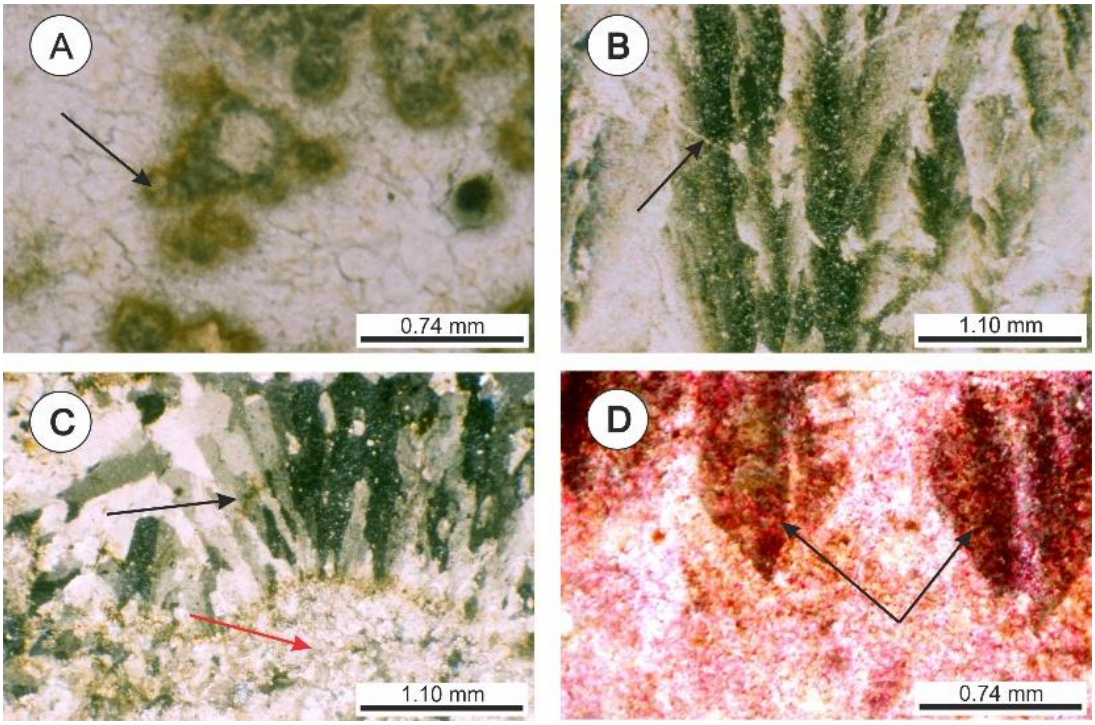

Figure 7. Photomicrographs of the Deir Alla travertines showing: **(A)** micritic clumps in the mottled texture and resembling shrub pustules (black arrow), the blocky (spar) cements are present as groundmass (red arrow) (sample № DA-26, non-stained, plane polarising light (PPL), x20); **(B)** long ray crystal shrub "feather calcite" expand upward (black arrow) (sample № DA-21, non-stained, cross polarising light (XPL), x4); **(C)** crystalline crust consists of spar crystals that have grown radially (black arrow) on the micritic basement (red arrow) and organised into bundles (sample № DA-20, non-stained, cross polarising light (XPL), x4); **(D)** dark brown radial spar crystals (more than 0.75 mm in radius) on the micritic basement (black arrows) (sample № DA-4, stained, cross polarising light (XPL), x20)

3.1.3. Stromatolite Travertine Microfacies

The Deir Alla travertines show stromatolites characterised by radial pairs of calcite about 0.8–1.2 mm in radius (Figure 8A; Table 1). Better development of one side of the ray and fan-like calcite crystals give a cedar tree appearance and intercalated microspar calcite (Figure 8B) with a gently convex stromatolite-like lamination with dark areas. The presence of visible dark areas is most probably related to organic matter or due to iron (Fe) enrichment (Figure 8C). Stromatolite-like lamination shows gently domed intercalation by columnar crystals growing from base to top (red arrow), with light-coloured ray calcite crystals overlying the stromatolite (Figure 8D), and appears wavy (Figure 9A).

The present travertine stromatolites were produced by the induration of biological felts, trapping and binding particles and precipitating minerals. Stromatolites are saline and freshwater microbial-laminated, organo-sedimentary structures common in various environmental settings and are produced by sediment trapping, binding, and low precipitation as a result of the growth and metabolic activity of algae microorganisms, principally cyanophytes (Freytet and Verrecchia, 2002).

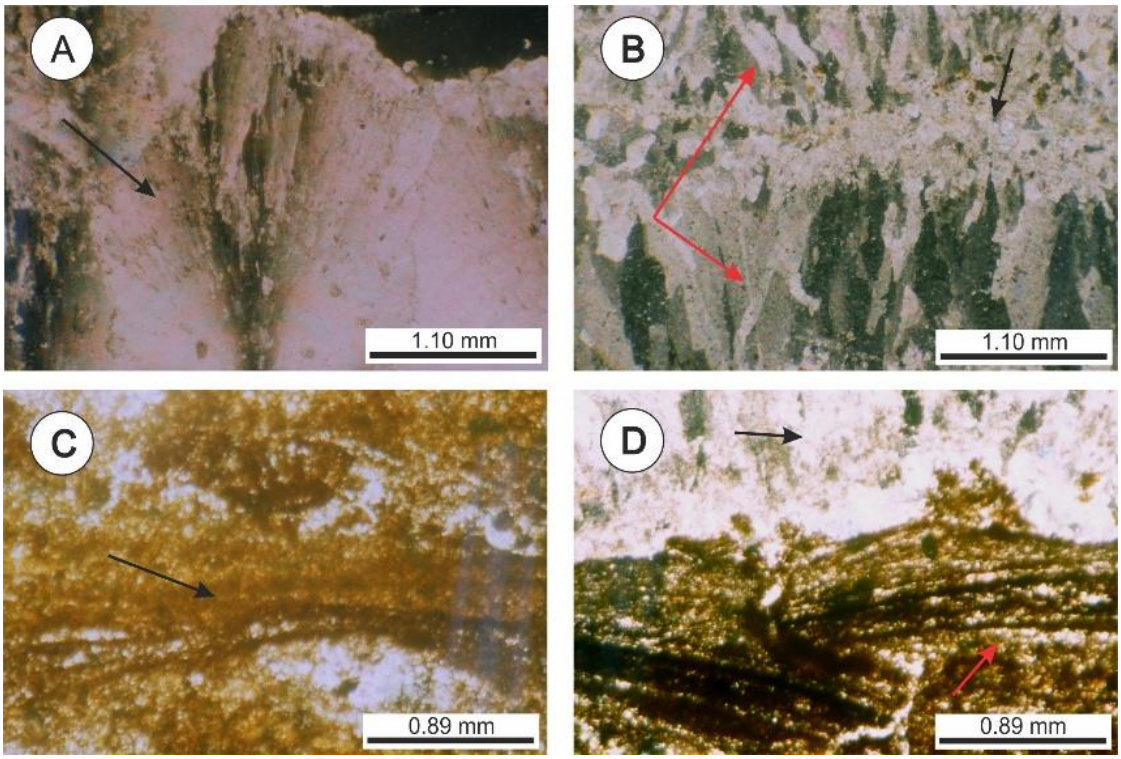

Figure 8. Photomicrographs of the Deir Alla travertines showing stromatolite microfacies characterised by: **(A)** radial pairs calcite about 0.8–1.2 mm in radius (sample № DA-26, non-stained, cross polarising light (XPL), x4); **(B)** better development of one side of ray and fan-like calcite crystals giving a cedar tree view (red arrows) and intercalated microspar calcite (black arrow) (sample № DA-8, non-stained, cross polarising light (XPL), x4); **(C)** Gently convex stromatolite-like lamination, note the presence of dark areas most probably related to organic matter or due to Fe enrichment (sample № DA-20, non-stained, cross polarising light (XPL), x10); **(D)** micro-non conformity stromatolite-like lamination, showing gently domed intercalated by columnar crystals growing from base to top (red arrow), light-coloured ray calcite crystals overlying the stromatolite (black arrow) (sample № DA-20, non-stained, cross polarising light (XPL), x10)

3.1.4. Peloidal Travertine Microfacies

Peloids are defined as regular, subspherical faecal grains ranging in size from 5 µm to 1 mm in diameter, and are usually associated with microorganisms. **A**ggregates of peloids form a clotted appearance with recrystallisation (Figure 9B), which is common in various bacteria and cyanobacteria (Croci et al., 2016); radial calcite crystals with small encrusting aragonite needles resemble the aragonite recrystallisation. This structure is similar to that of the Deir Alla peloids. The peloids were found in the upper part of the Deir Alla section (i.e., it resembles a pond sub-environment). These peloids are cryptocrystalline, pale-dark green in colour, elliptical to spherical in shape, and are less than 0.25 mm in diameter. Clotted mesofabric structures are referred to as thrombolites and rarely occur in lakes, according to Riding (2000) and Pache et al. (2001).

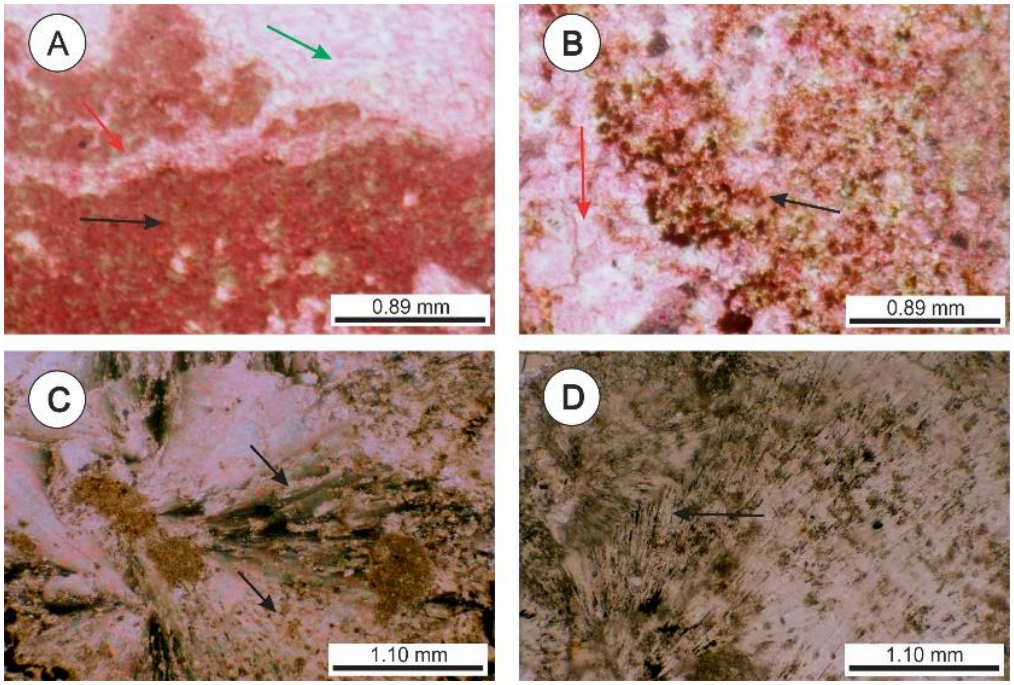

Figure 9. Photomicrographs of the Deir Alla travertines (Stromatolite Microfacies and Peloidal Microfacies) showing: **(A)** stained stromatolite-like wavy lamination of thicker micrite, recrystallisation present in the upper right corner (green arrow) (black arrow) and thinner sparite (red arrow) laminae (sample № DA-23, stained, Plane polarising light (PPL), x10); **(B)** aggregates of peloids form clotted appearance, recrystallisation seen in the lower left corner (red arrow) (sample № DA-4, stained, cross polarising light (XPL), x10); **(C)** radial calcite crystals with small encrusting aragonite needles (black arrow) that resembling the aragonite recrystallisation (sample № DA-26, non-stained, cross polarising light (XPL), x4), note the aggregates of peloids form a clotted appearance; **(D)** close-up view (9-C) for more details (black arrow) (sample № DA-26, non-stained, cross polarising light (XPL), x4), note the aggregates of peloids form a clotted appearance

3.2. Microfacies of the Suwayma Travertines

The Suwayma travertines are exposed along the north-eastern margin of the Dead Sea shoreline. They are cream-coloured and 78 m thick (Figures 1 and 2; Table 1). The measured section unconformably and partially overlies the Lisan Marl Formation and the Pleistocene basalt, and is overlain by Recent alluvial sediments. Therefore, the travertine deposits are younger than the basalt occurrences and contain detrital basaltic inclusions. Most of the travertines are hard, micritic, whitish-yellowish to reddish in colour, root-rich, and exhibit abundant vuggs (Al-Thawabteh et al., 2006).

The petrographic characteristics of the Suwayma travertine microfacies are not very different from those of the Deir Alla travertines. These travertines are mainly composed of crystalline crusts, shrubs, stromatolites, peloids, ooids, and flora.

3.2.1. Crystalline Crust Travertine Microfacies

The SEM (FEI Quanta 600) observations of the upper part of the Suwayma strata display a wide range of calcite morphology. They include rhombic and other scalenohedral crystals (Figure 10A). Some crystals appear as well-developed rhombs (Figure 10B). The most common type

of structure is the presence of individual patches composed of an aggregate of rounded nanometre-scale crystallites at the surface of larger blocky calcite crystals (Figure 10C). The cement in the Suwayma travertines is represented by a mass of seedy calcite crystals mantling the travertine samples (Figure 10D; Table 1).

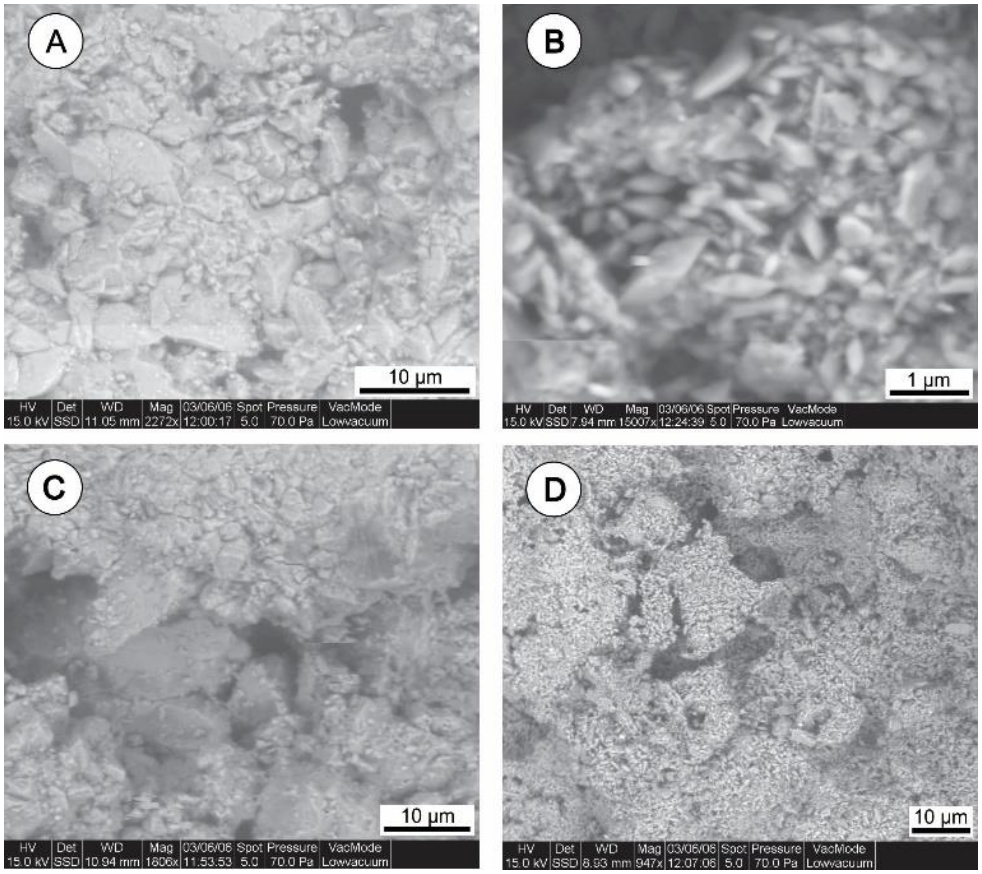

Figure 10. SEM images of the Suwayma travertines showing Crystalline Microfacies: **(A)** calcite rhombs and other composite scalenohedral crystals occurring in the upper part of the Suwayma section (sample № SW-32 and Mag. 227x); **(B)** well-developed calcitic rhombs (sample № SW-45 and Mag. 1507x); **(C)** individual patches of aggregate of rounded nanometre-scale crystallites at the surface of larger blocky calcite crystals (sample № SW-32 and Mag. 1806 x); **(D)** later cement was formed from seedy calcite crystals (sample № SW-45 and Mag. 947x).

Under the polarising microscope, calcite is mainly present as micrite (Figure 11A) and sparite groundmass (Figure 11B). Secondary spar calcite fills the cavities and appears as a drusy texture (Figure 11C), similar to the ones reported by Claes et al. (2015, 2017). The presence of quartz grains is more common than in the Deir Alla travertines. They occur as small anhedral-subhedral crystals, monocrystalline to some polycrystalline, corroded, subrounded and mainly coated with iron oxide and/or clay minerals (Figures 11D and 12A). The clay minerals appear whitish to greenish in colour in the Suwayma section, mainly coated with detrital quartz grains (Figure 11D).

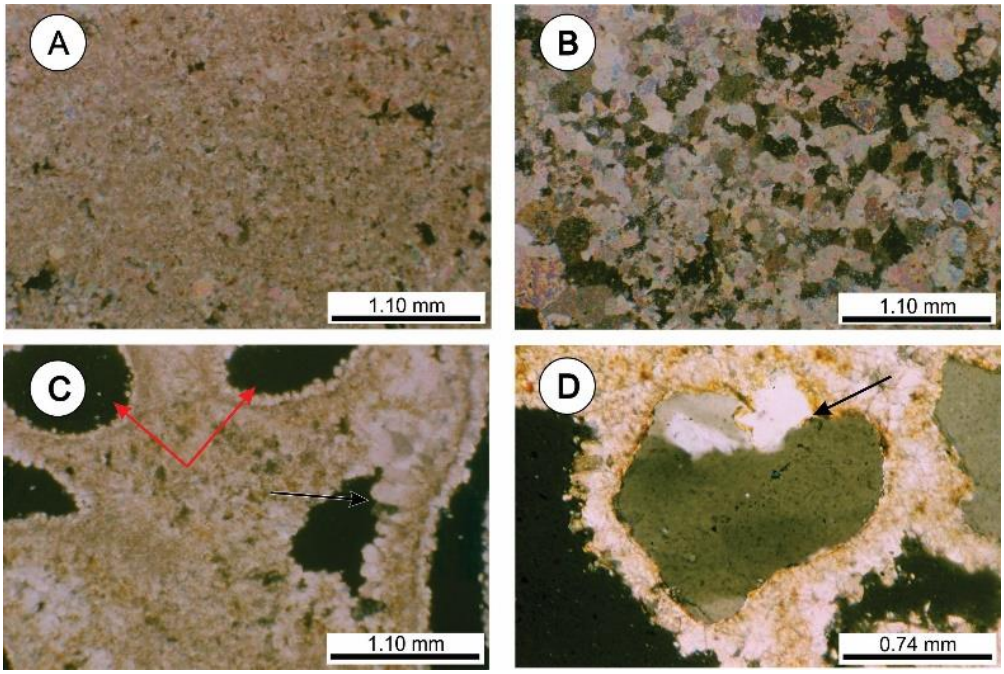

Figure 11. Photomicrographs of the Suwayma travertines showing Crystalline Crust Microfacies: **(A)** micrite groundmass (sample № SW-34, non-stained, cross polarising light (XPL), x4); **(B)** microsparite-macrosparite groundmass (sample № SW-36, non-stained, cross polarising light (XPL), x4); **(C)** cavities formed in micrite groundmass (red arrows), and coated with spar calcite crystals that increased toward the centre, which resemble an isopachous cement (black arrow) (sample № SW-27, non-stained, cross polarising light (XPL), x4); **(D)** subrounded, embayment texture (black arrow), coated with iron oxide, appears corroded, and coated with polycrystalline quartz grains (sample № SW-49, non-stained, cross polarising light (XPL), x 20)

Most of the studied samples contain iron, probably as amorphous oxides, mainly hematite and limonite. These oxides form diffused masses within the calcitic groundmass (Figure 12B); iron compounds also coat cavities. Iron (Fe) solutions seem to intrude into the calcite groundmass and destroy the lamination (Figure 12C).

A few dolomites and high-iron dolomites (ankarite) were identified under the microscope (Figure 12D). The stromatolite-like laminations were observed in the field, but no thin sections were prepared. The iron oxides (Fe_2O_3) increase slightly toward the top of the Suwayma section.

The iron-rich (Fe) travertine is similar to the active hydrothermal systems elsewhere as thermogenic travertines, with variable changes relative to their distal-proximal location from water flow, vent, duration of aerial exposure, and natural redox conditions (Kanellopoulos et al., 2018).

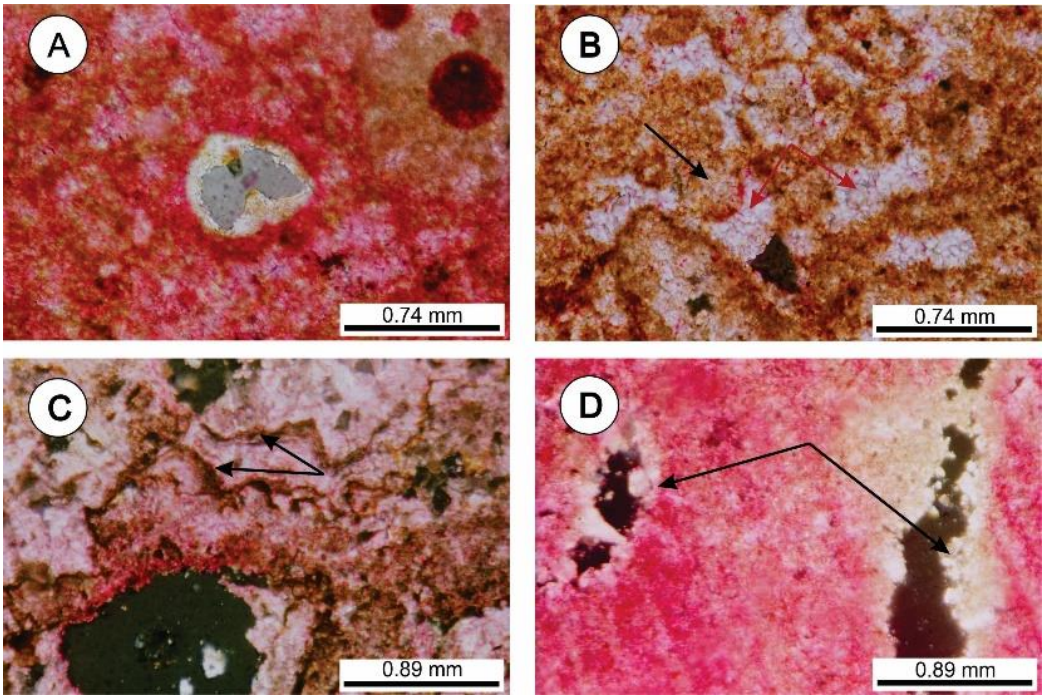

Figure 12. Photomicrographs of the Suwayma travertines showing: **(A)** small, subrounded, detrital, coated with clay mineral, corroded and monocrystalline quartz grain (sample № SW-37, stained, cross polarising light (XPL), x20); **(B)** iron-rich calcite (black arrow), and rhomb dolomite crystals clear in non-stained areas (red arrows) (sample № SW-47, stained, cross polarising light (XPL), x20); **(C)** distorted iron-rich laminae (black arrows) (sample № SW-39, stained, cross polarising light (XPL), x10); **(D)** dolomite crystals coated the cavities (black arrows), which resemble drusy cement (sample № SW-34, stained, cross polarising light (XPL), x10)

3.2.2. Shrub Travertine Microfacies

Shrub travertines were observed in the lower and upper parts of the Suwayma section (Figure 13A). Their descriptions are similar to those described in the Deir Alla section.

3.2.3. Stromatolite Travertine Microfacies (SW-8)

These stromatolites have an organosedimentary structure, trapping, binding, and low precipitation; and show the metabolic activity of algae. Such stromatolites are similar to those in the Deir Alla area.

3.2.4. Peloids Travertine Microfacies

Peloids are common in the Suwayma travertines. They are dark-green in colour, cryptocrystalline to microcrystalline carbonates of spherical and ellipsoidal shape, with less than 1 mm in diameter, and do not appear as clotted peloids. Some of them are rich in iron (Fe) content (Figure 13B, C; Table 1).

3.2.5. Ooids Travertine Microfacies

Ooids are coated grains that grow in shallow water saturated with calcium carbonate and are found in the travertine system, where currents and

agitations are common. They are spherical to elliptical grains, 0.25 to 2.00 mm in diameter, with a nucleus and a radial or concentric structure, similar to those described by Claes et al. (2015, 2017) and Croci et al. (2016). The cortex of an ooid exhibits smooth and even coatings, especially in the outer films. In the lower part of the Suwayma section, the light to dark green ellipsoidal ooids are composed of single cortices associated with bacterial clumps displaying branching and radiating forms almost perpendicular to the ooid surface, exhibiting a shrub-like shape (Figure 13D).

Furthermore, the ooids in the Suwayma travertines can be identified as spheroidal shaped calcite grains, ranging from 1–2 mm in diameter. Some of the ooids' nuclei consist of quartz grains (Figure 14A; Table 1). In some cases, two ooids grow together, as shown in Figure (14B). Light and dark concentric laminae of ooid grains developed around two nuclei (Figure 14C). A close-up view in Figure 14C shows irregular cortices of the dark micrite and light sparite (Figure 14D).

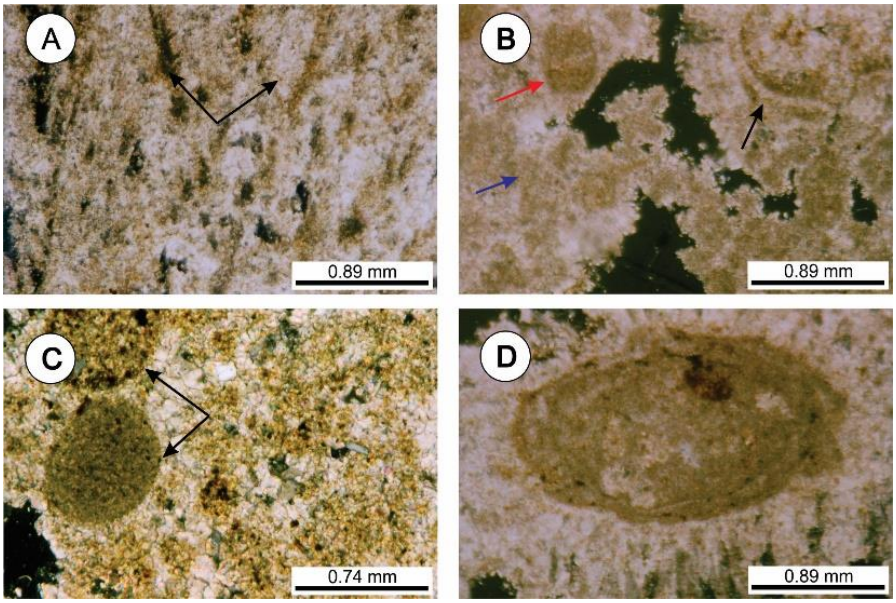

Figure 13. Photomicrographs of the Suwayma travertines showing (Shrubs, Ooids, Peloids, and Oncoids): **(A)** shrub travertine (black arrows) (sample № SW-39, non-stained, plane polarising light (PPL), x10); **(B)** peloids (red arrow), and alternated micrite and sparite laminae in a fan-like growth (black arrow) (sample № SW-10, non-stained, cross polarising light (XPL), x10); **(C)** dark-green pairs of spherical peloids formed in microspar calcite groundmass (black arrows), spar crystals under the micritic clumps' support resemble the recrystallisation of micrite (blue arrows) (sample № SW-49, non-stained, cross polarising light (XPL), x20); **(D)** elliptical ooid that has a clear nucleus and associated with bacterial branching clumps, which occur in a radial pattern almost perpendicular to the surface showing a shrub-like form (sample № SW-10, non-stained, cross polarising light (XPL), x10)

3.2.6. Oncoids Travertine Microfacies

Oncoids are concentrically laminated travertines with an irregularly laminated cortex. Oncoids are present in travertines deposited in streams and lakes. Light to dark green irregular or spheroidal oncoids consist of irregular, frequently overlapping and intersecting concentric laminae (Figure 15A).

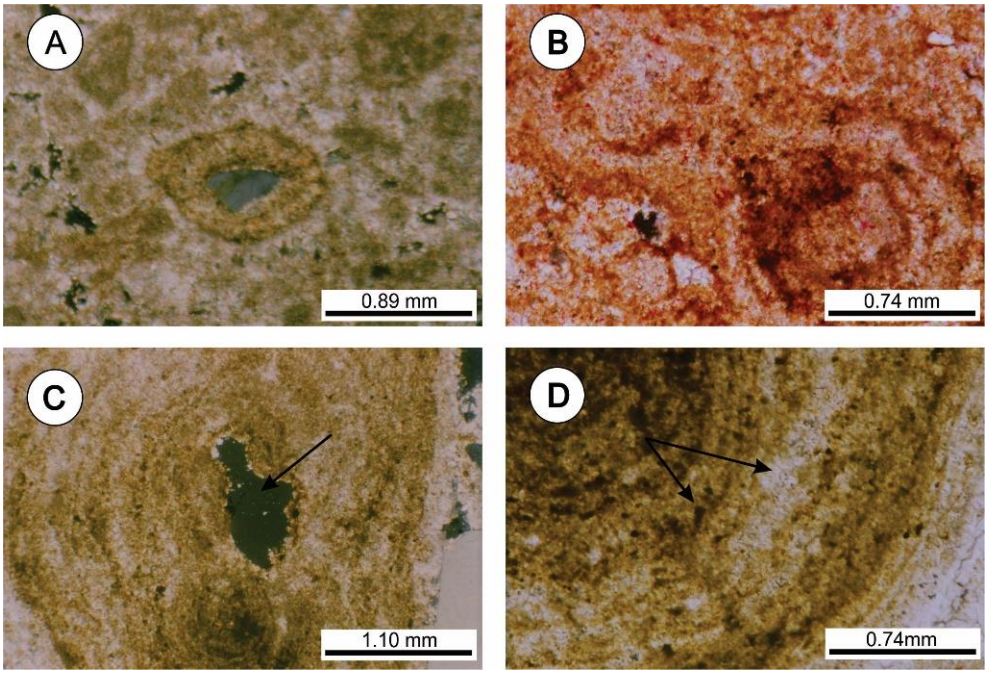

Figure 14. Photomicrographs of the Suwayma travertines (Ooids) showing: **(A)** elliptical ooids possessing regular concentric laminae developed around quartz nuclei (sample № SW-10, non-stained, cross polarising light (XPL), x10); **(B)** two ooid grains grow together (sample № SW-47, stained, cross polarising light (XPL), x20); **(C)** light and dark concentric laminae of ooid grains developed around two nuclei, the upper one is missed (black arrows) (sample № SW-22, non-stained, cross polarising light (XPL), x4); **(D)** close-up view of **(13-C)** showing the irregular cortices of dark micrite and light sparite (sample № SW-22, non-stained, plane polarising light (PPL), x20)

3.2.5. Spores Travertine Microfacies

Travertines commonly contain rich flora components comprising leaf impressions, encrustations, and coatings of moss cushions, twigs, seeds, and pollen. Flora identification, especially of tree types, is useful for constructing and supporting other evidence found to elucidate the palaeoenvironmental setting (Pentecost, 2005; Della Porta, 2015). The flora observed in the upper part of the Suwayma section is identified as Charophyte oospores (gyrogonites) (Soulié-Märsche and García, 2015) (Figures 15B and 15C; Table 1). Generally, Charophyte oospores (gyrogonites) have often been recorded in temporary Pleistocene lacustrine conditions (Pentecost, 2005). Along the slopes of Suwayma, Charophyte flora is common in the terraced-like areas. The areas are concomitant with the lake Lisan terraces described by Abu Ghazleh and Kempe (2009) along the eastern coast of the southern Dead Sea. Such terraces served as travertine depositional settings for pond reconstructions (Croci et al., 2016). In a tectonic regime with faults, they acted as fluid paths for thermal water, which was responsible for travertine precipitation (Croci et al., 2016).

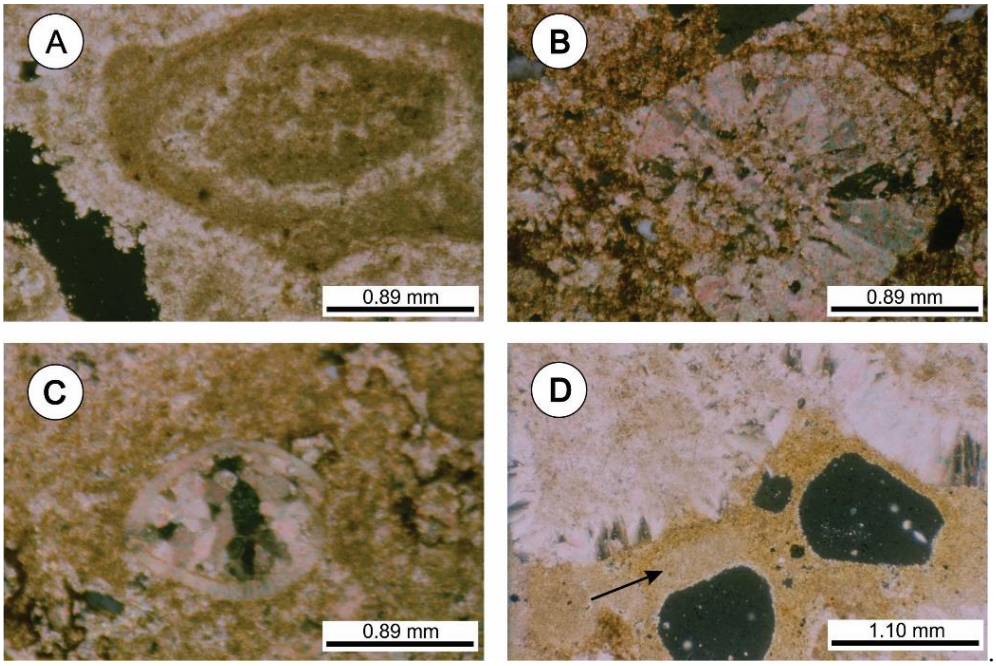

Figure 15. Photomicrographs of the Suwayma travertines showing (Oncoids and flora): **(A)** elliptical oncoids, note the irregular concentric laminae developed around semi-clear nuclei (sample № SW-10, non-stained, cross polarising light (XPL), x10); **(B)** Charophyte oospores (gyrogonites) were infilled with fan-like calcite crystals (sample № SW-1, non-stained, cross polarising light (XPL), x10); **(C)** Charophyte oospores (gyrogonites) were infilled with spar calcite (sample № SW-37, non-stained, cross polarising light (XPL), x10); **(D)** microcrystalline cement infilled the pore space (black arrow) (sample № SW-45, non-stained, cross polarising light (XPL), x4)

3.3. Microfacies of the Az Zara Travertines

3.3.1. Crystalline Crust Travertine Microfacies

The Az Zara travertines are mineralogically similar to the samples from Deir Alla and Suwayma. The studied samples are also composed of calcite without any indicated presence of quartz. The SEM images of the lower part of the Az Zara samples display a wide range of arrangements of calcite crystals in crystalline crust microfacies (Figures 16A, 16B, and 16C; Table 1). Rhombic and other scalenohedral composite crystals occur (Figure 16A). Some of these crystals appear as well-developed rhombs. The most common type of calcite crystal is circular calcite, which is composed of small trigonal prisms with convex faces. Circular calcite crystals are mainly associated with calcified rods of the bacilliform bacteria (Figure 16B).

3.3.2. Stromatolite Travertine Microfacies

The stromatolite-like structures (Figure 16D) are similar to those previously described in the Deir Alla petrographic section.

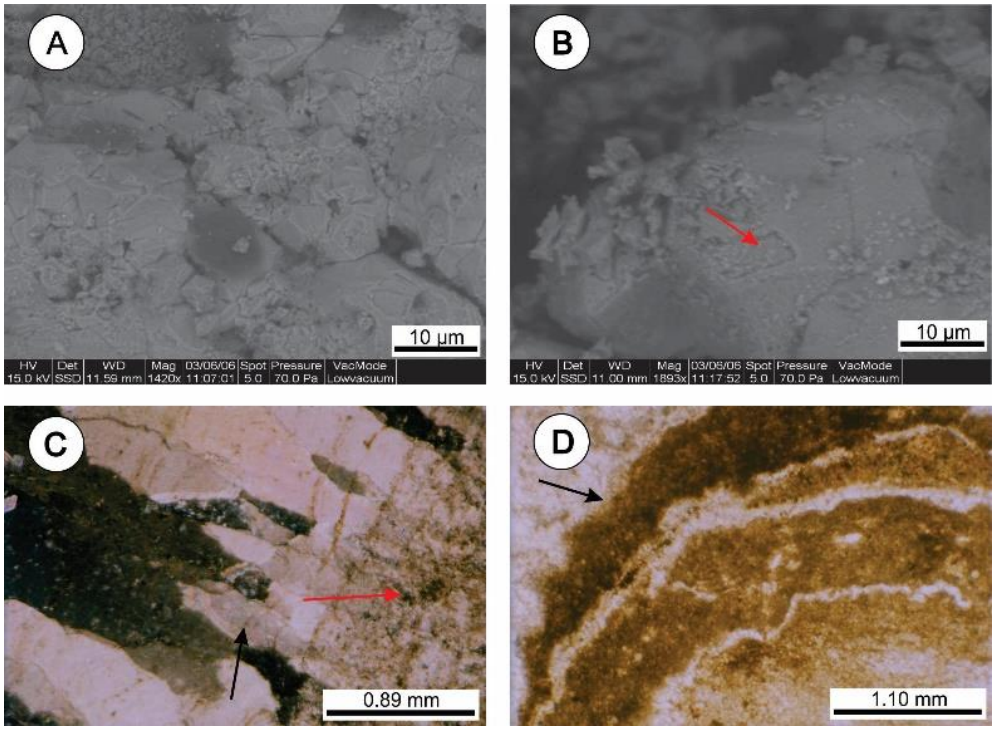

Figure 16. SEM images and photomicrographs of the Az Zara travertines (Crystalline Crust Microfacies) showing: **(A)** SEM image shows rhomb calcites and other composite of circular crystals in the lower part of the Az Zara section (sample № AZ-1 and Mag. 1420x); **(B)** SEM image shows circular calcite crystals with minute crystallites (black arrow). These crystallites are probably calcified rods of the bacilliform bacteria, note the shield-like calcite crystals in some places cover the circular calcites (red arrow) (sample № AZ-1 and Mag. 1893x); **(C)** photomicrograph of crystalline crust consists of ray and fan-like calcite crystals (black arrow) overlaying the micrite basement (red arrow) (sample № AZ-3, non-stained, cross polarising light (XPL), x10); **(D)** photomicrograph of domed, wavy, stromatolite-like structure consisting of alternation of organic matter-rich micrite laminae and light microspar calcite (black arrow) (sample № AZ-4, non-stained, plane polarising light (PPL), x4)

The micrite and spar calcite appear as groundmass in all samples. The boundaries of spar calcite crystals resemble other compaction types (Figures 17C and 17D). A few grains of quartz are present as small subhedral-euhedral crystals, monocrystalline, corroded, rounded and mainly coated with iron oxides (Fe_2O_3).

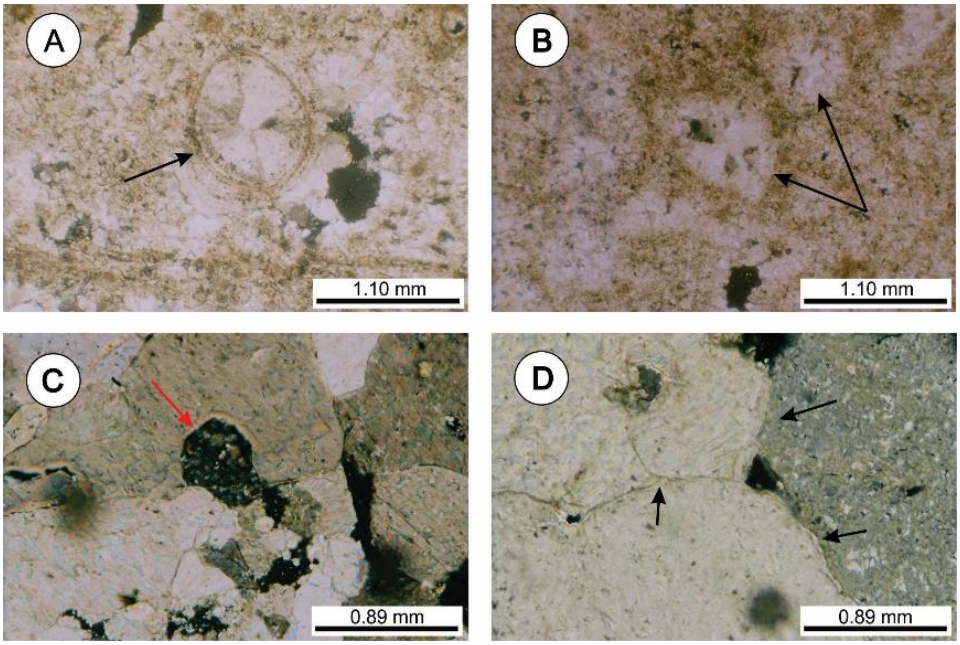

Figure 17. Photomicrographs of the Az Zara travertines (Crystalline Crust and Flora microfacies) showing: **(A)** Charophyte oospores (gyrogonites) preserved the morphology of the woody tissues (black arrow) (sample № AZ-4, non-stained, cross polarising light (XPL), x4); **(B)** Charophyte oospores (gyrogonites) unpreserved the morphology of the woody tissues (black arrows) (sample № AZ-4, non-stained, cross polarising light (XPL), x4); **(C)** embayment texture of calcite crystals (red arrow), and zoning calcite (black arrow) (sample № AZ-1, non-stained, cross polarising light (XPL), x10); **(D)** planar grain-to-grain contact occurred between calcite crystals (black arrows) (sample № AZ-1, non-stained, cross polarising light (XPL), x10)

Iron is formed as circular and diffused masses within the calcitic groundmass (Figure 18C; Table 1). Iron oxides (Fe_2O_3) form part of the stromatolites and peloids and coat the cavities (Figure 18D). The wide distribution of iron oxides as gaps infilling and cavities rimming is the result of the iron oxide-rich fluid circulation during the diagenesis of travertines (Claes et al., 2015, 2017). The clay minerals appear as whitish to greenish in thin sections.

The ferruginous ooid encompasses an iron oxide-coated grain nucleus (Bhattacharyya and Kakimoto, 1982). The iron crust coated grains from the ferruginous oolitic limestone microfacies are brown in colour and spheroidal to elliptical in shape. Commonly, iron occurs as irregularly distributed among the laminae and voids and is occasionally replaced by carbonate, which infills the gaps and rimming cavities during the diagenesis processes.

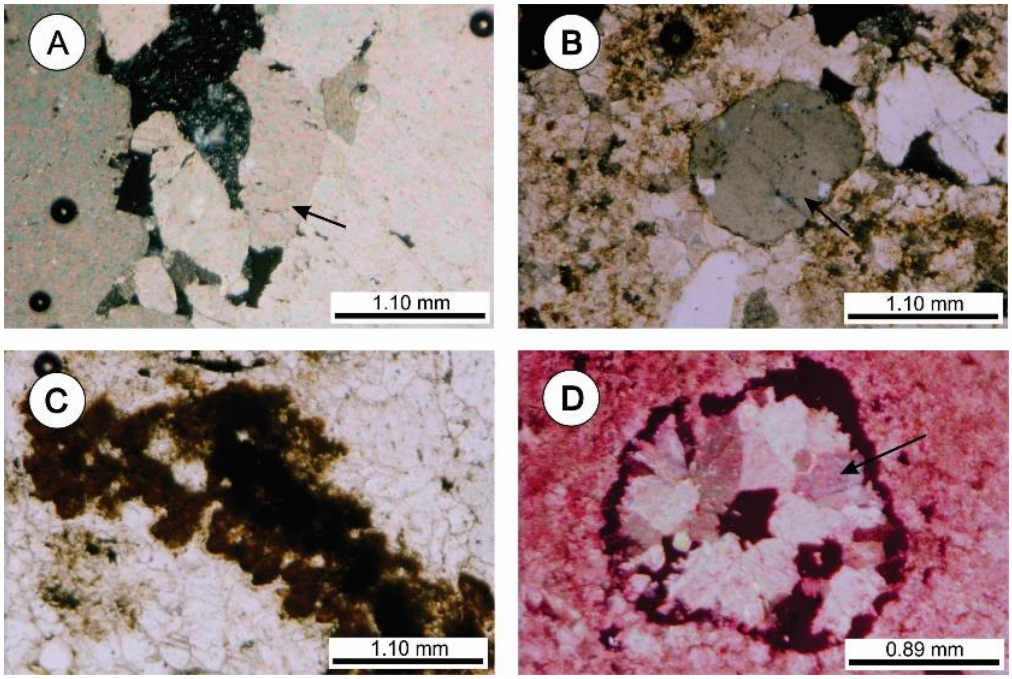

Figure 18. Photomicrographs of the Az Zara travertines (Crystalline Microfacies) showing: **(A)** Fan-like calcite crystals cluster (black arrow) (sample № AZ-1, non-stained, cross polarising light (XPL), x4); **(B)** rounded quartz grain bounded by iron oxide (black arrow) (sample № AZ-1, non-stained, cross polarising light (XPL), x4); **(C)** circular and diffuse iron oxides are mainly hematite (sample № AZ-1, non-stained, plane polarising light (PPL), x4); **(D)** cavity was coated with iron oxides and infilled with spar calcite crystals that increased in size toward the centre (black arrow) (sample № AZ-3, stained, cross polarising light (XPL), x10).

3.3.3. Spores Travertine Microfacies

The spores' observations Charophyte oospores (gyrogonites) are similar to those described in the Suwayma petrographic section (Figures 17A and 17B).

The original stems and twigs are generally not preserved, but their mouldic pores are infilled with calcite spar or micrite that preserve the tissue morphic shape (Figures 19A and 19B). Calcite spar palisades and micrite are developed with bush-like forms, which may also display diffused thin laminae, with filaments cutting lamination (Figure 19B).

The described macrophyte encrustation structures probably represent algae, cyanobacteria, or bryophytes. Nevertheless, some of the laminae are probably abiotic in origin because of the absence of organic remains or traces.

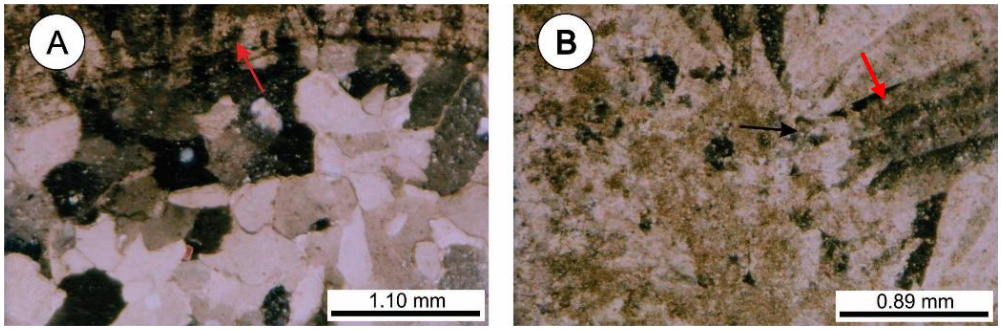

Figure 19. Photomicrographs of the Az Zara travertines showing: **(A)** blocky calcites infill the stem and preserve the morphology of the wood tissues (red arrow) (sample № AZ-3, non-stained, cross polarising light (XPL), x4); **(B)** shrubs occur as spar calcite and microspar, take bush-like shapes, passing through the dark micrite (black arrow) with filaments (red arrow) (sample № AZ-3), non-stained, cross polarising light (XPL), x10)

3.3.4. Shrub Travertine Microfacies

Shrubs occur as spar calcite and microspar, take bush-like shapes, passing through the dark micrite with filaments, similar to those described in the Deir Alla section.

4. DISCUSSION

The present study of Jordan's travertines reveals that most investigations are related to meteoric diagenesis, which provides the required cementation, sparmicritization, neomorphism, and dissolution. The form of many cement crystals can be indicative of the environment in which they grew. Blocky and mosaic cements were recognised in travertines. The blocky cement is considered equidimensional cementing crystals, forming in meteoric phreatic or burial phreatic environments. The mosaic (drusy) cements are identified by the cavities infilled with calcite crystals, which increase in size toward the centre of the cavities. The development of calcite crystals is mostly related to the meteoric phreatic environment in which the degree of carbonate saturation and/or fluid flow is low (Chafetz and Folk, 1984; Chafetz and Guidry, 1999).

Kahle (1977) defined the term "sparmicritization" as the destructive activities of microorganisms etching spary carbonate rocks. This process is observed as spar crystals under the micritic clumps (Figures 4D and 7A), and these spars are in the process of being micritised. Kahle (1977) considered this process as micritization, formed by the dissolution-crystallization of the spar crystals.

Aggradational neomorphism is the recrystallisation process by which micrite transforms to sparite *in situ* (Love and Chafetz, 1988, 1990). This form of diagenesis is common in algal travertines (Figures 4C, 9A, and 9B) (Claes et al., 2015, 2017). The Suwayma crystalline crust microfacies indicate a depositional environment with fissure slopes and smooth slopes. It is evident that crystalline crust can likely develop in high water flow velocity conditions where biogenic activity is weak (Guo and Riding, 1998). The development of radial calcite crystals is the result of contemporaneous crystallisation from hot water. Light and dark laminated alternations are due to diurnal variation near the spring area (Folk et al., 1985; Guo and Riding, 1998).

Some travertines are deposited initially as aragonite; neomorphism subsequently takes place. When recrystallisation of aragonite takes place, it transforms into calcite due to its higher solubility and microcrystalline form. The interbedded conglomerate-brecciated facies (Figure 2) is commonly composed of travertine fragments. The presence of travertine fragments associated with crystalline crusts is similar to the intraformational breccias described by Pola et al. (2013), stating that travertine fragments were precipitated near to the discharge point.

Iron-rich travertine precipitates in Deir Alla are common in shrub travertine microfacies and display dark-coloured micritic shrub forms that expand upward and are enriched by iron oxides (Figure 6D). They are also common in stromatolite travertine microfacies, which occur as gently convex stromatolite-like laminations possessing dark areas due to organic matter or iron (Fe) enrichment (Figure 8C). Iron-precipitates are also common in the Suwayma travertines as those associated with the crystalline microfacies show sub-rounded, embayment texture coated with iron oxide corroded and polycrystalline quartz grains (Figure 11D). Dendritic texture shows an internal branching growth pattern similar to that described by Claes et al. (2017), which is either crystalline or consists of knob-shaped micritic aggregates. Ooids and oncoids show iron-rich calcite and rhomb dolomite crystals clearly in non-stained areas (Figure 12A) and distorted iron-rich laminae (Figure 12C). At Az Zara, the travertine crystalline microfacies show a domed, wavy stromatolite-like structure consisting of an alternation of iron-rich micrite laminae and light microspar calcite (Figure 16D), rounded quartz grains bounded by iron oxide (Figure 18B), and circular and diffuse iron oxides that are mainly hematite (Figure 18C), as well as cavities coated with iron oxides and infilled with spar calcite crystals that increase in size toward the centre (Figure 18D).

Mineralogical, geochemical, and sedimentological data of the ferruginous coated grains in the investigated travertines in Jordan provide a thorough understanding of their depositional environment around the vents and rivulets (Ibrahim et al., 2017). Petrographic microscopy was used to determine the microfacies morphology of coated grains (Reolid et al., 2008).

It is evident that trapping and binding sediments alone will not give rise to the lamination of stromatolites. Therefore, lamination generation requires periodic interruption to trapping and binding skeletal and lithic fragments to form micritic lamina (Visscher et al., 2000; Dupraz et al., 2009). Macintyre et al. (2000) indicated that the lithified laminae in modern marine stromatolites in the Bahamas are the result of the microboring activity of endolithic cyanobacteria, associated with low rates of sedimentation. Microbial deposition in pools is influenced by bathymetry, water energy, and physiographic features that control stromatolite growth and sedimentation. Stromatolites were also laid down at the lakes and channel margins where trapping of clastic materials took place. Stromatolite morphology and structure are affected by the environment if the physical forces are strong, whereas the biological communities play the main role when physical forces are weak (weak water energy, weak currents, and low gradient) (Suosaari et al., 2019;

Claes et al., 2015, 2017). Trapping, binding, low precipitation, and metabolic activity of algae and cyanophytes are favourable to the deposition of stromatolite microfacies.

The presence of the shrub microfacies in Deir Alla indicates deposition in terrace pools, shallow and low-angle slope pools of warm water. The crystalline crust is deposited in a high flow velocity of water on smooth slopes (Folk et al., 1985), terraced slopes, pool rims, and vertical walls. According to Chafetz and Folk (1984) and Pentecost (1990), shrub layers indicate growing seasons (spring–summer), whereas micritic layers represent the non-growing season (winter). Bacterial shrubs are formed from warm water (Chafetz and Folk, 1984; Pentecost, 1990; Chafetz and Guidry, 1999). Therefore, shrub forms are not found in cool water travertines.

Similar Charophyte spores to those observed in the upper part of the Suwayma and Az Zara sections were recorded by Evans (1999), who described the Charophyte oospores (gyrogonites) as a common feature of the lacustrine tufa and interpreted it as a low-energy bench-type carbonate pond. According to Hasan and Chakrabarti (2009), macrophytes are common in different kinds of water bodies, such as estuaries, rivers, floodplains, lakes, ponds, and swamps. Macrophytes always occur as algae, floating macrophytes, submerged macrophytes, and emergent macrophytes.

Peloids, ooids, and oncoids: the deposition of ooids indicates that calcium carbonate saturated the shallow water warm springs in a travertine's high hydrodynamic energy depositional environment. For the spore microfacies to develop, lacustrine conditions, dammed lakes, low-energy bench-type carbonate ponds, and terraced-like areas are required. The Az Zara crystalline crust microfacies were deposited on a smooth slope with self-built channels. Reeds and other macrophyte encrustations require the fluvio-palustrine depositional setting.

Dendritic texture shows an internal branching growth pattern similar to that described by Claes et al. (2017), which is either crystalline or consists of knob-shaped micritic aggregates. The interbedded paleosol horizons (Figure 2) are commonly composed of travertine fragments and claystone that precipitated near the discharge points as breccia. The presence of travertine fragments associated with crystalline crusts is similar to the intraformational breccias described by Pola et al. (2013).

5. CONCLUSIONS

The investigation of the travertine microfacies associations reveals variable diagenetic processes including cementation, dolomitisation, and neomorphism, which acted as the main meteogene and burial diagenetic features that affected the studied travertines. Three types of cement were recognised, namely the mosaic, isopachous, and overgrowth types of cement. The mosaic cement is similar to that described in the Deir Alla travertines. In the lower part of the Suwayma section, the travertine contains fine-grained microcrystalline cement infilling the pore spaces. Isopachous cement, observed as a layer of spar calcite crystals, retains a constant thickness. Recrystallisation of micrite into sparite is common in the Suwayma travertines.

The bacterial and algal activity is probably the source of this aggraded micrite. Sparmicritization is observed

in the Suwayma travertines, where spar crystals are found under the micritic clumps. Therefore, it is assumed that spars become micritised due to biotic and abiotic processes.

Dolomitisation resulting from available magnesium-enriched (Mg) solution could lead to complete replacement and loss of organic matter, while pressure-solution could lead to dissolution and recrystallisation. Dolomitisation is classified as one type of burial diagenesis that takes place in buried travertines under several metres of overburden or more. Dolomitisation in the Suwayma travertines does not exceed 2%, occurring around the cavities in those beds covered by several metres of travertine. These observations indicate that magnesium-enriched (Mg) solution passes throughout the pre-existing travertines and leads to the replacement process.

Future research on Jordan's Late Pleistocene travertines should consider the vast exposures along the Dead Sea–Jordan Valley setting in terms of vertical and lateral stratigraphic relationships as well as the morphological features that characterise the travertine outcrops.

6. ACKNOWLEDGEMENTS

The authors are greatly indebted to the Deanship of Research and Graduate Studies at Hashemite University for research grant support through the project entitled "Genesis and Palaeo Environmental Significance of Hot Spring Travertines in Jordan." This paper is based on the unpublished M.Sc. thesis prepared by Sana' Al Thawabteh under the supervision of the first and second authors. Great thanks to Eng. Qais Al-Qaisie, the Director of the Travco Company, who granted fieldwork access to study the travertines at the company's site at Deir Alla. The authors would like to thank Tareq El-Beshetie for assisting with sample preparation and rock cutting work, as well as Reem Al-Shueibi for drafting the paper. Two anonymous reviewers are greatly thanked for their helpful comments.

7. REFERENCES

Abu Ajamieh, M. (1980). The Geothermal Resources of Zarqa Ma'in and Zara. Amman, Jordan.

Abu Ghazleh, S., Kempe, S. (2009). Geomorphology of Lake Lisan terraces along the eastern coast of the Dead Sea, Jordan. Geomorphology: 108, 246–263.

Al-Thawabteh, S.M. (2006). Sedimentology, Geochemistry, and Petrographic Study of Travertine Deposits along the Eastern Side of the Jordan Valley and Dead Sea Areas. Master's Thesis, Hashemite University, Zarqa, Jordan.

Bhattacharyya, D.P., Kakimoto, P.L. (1982). Origin of ferriferous ooids: a SEM study of ironstone ooids and bauxite pisoids. J. Sedimentary Petrology: 52, 849–857.

Capezzuoli, E., Gandin, A., Pedley, M. (2014). Decoding tufa and travertine (fresh water carbonates) in the sedimentary record: The state of the art. Sedimentology: 61, 1–21. doi: 10.1111/sed.12075

Chafetz, H. S., Folk, R. L. (1984). Travertine: Depositional morphology and the bacterially constructed constituents. Sedimentary Petrology: 54, 289-316.

Chafetz, H. S., Guidry, S. A. (1999). Bacterial shrubs, crystal shrubs, and ray-crystal crusts: Bacterially induced vs a biotic mineral precipitation, Sediment. Geo: 126, 57-74.

Claes, H., Soete, J., Van Noten, K., El Desouky, H., Marques Erthal, M., Vanhaecke, F., Ozkul, M., Swennen, R. (2015). Sedimentology, three-dimensional geobody reconstruction and carbon dioxide origin of Pleistocene travertine deposits in the Ballık area (south-west Turkey). Sedimentology 62(5): 1408-1445. http://dx.doi.org/10.1111/sed.12188.

Claes, H., Erthal, M.M., Soete, J., Ozkul, M., Swennen, R. (2017). Shrub and pore type classification: Petrography of travertine shrubs from the Ballık-Belevi area (Denizli, SW Turkey). Quaternary International 437: 1-17. DOI: 10.1016/j.quaint.2016.11.002

Croci, A., Della Porta, G., Capezzuoli. E. (2016). Depositional architecture of a mixed travertine-terrigenous system in a fault-controlled continental extensional basin (Messinian, Southern Tuscany, Central Italy). Sedimentary Geology 332: 13-39.

Della Porta, G. (2015). Carbonate build-ups in lacustrine, hydrothermal and fluvial settings: comparing depositional geometry, fabric types and geochemical signature. Geological Society, London, Special Publications 418: 17-68, https://doi.org/10.1144/SP418.4.

Della Porta, G., Croci, A., Marini1, M., Kele, S. (2017a). Depositional Architecture, Facies Character and Geochemical Signature of the Tivoli Travertines (Pleistocene, Acque Albule Basin, Central Italy). Rivista Italiana di Paleontologia e Stratigrafia (Research in Paleontology and Stratigraphy) 123(3): 487-540.

Della Porta, G., Capezzuoli, E., De Bernardo, A. (2017b). Facies character and depositional architecture of hydrothermal travertine slope aprons (Pleistocene, Acquasanta Terme, Central Italy). Marine and Petroleum Geology 87: 171-187. https://doi.org/10.1016/j.marpetgeo.2017.03.014.

Dupraz, C., Reid, R. P., Braissant, O., Decho, A. W., Norman, R. S., Visscher, P. T. (2009). Processes of carbonate precipitation in modern microbial mats. Earth-Science Reviews 96: 141.

Evans, J. E. (1999). Recognition and implications of Eocene tufas and travertines in the Chadron Formation, White River Group, Badlands of South Dakota. Sedimentology 46: 771-789.

Folk, R. L., Chafetz, H. S., Tiezzi, P. A. (1985). Bizarre forms of depositional and diagenetic calcite in hot springs travertines, Central Italy. In: Schneidermann, N. and Harris, P. (editors), Carbonate Cements. Society of Economic Paleontologists and Mineralogists, Special Publication: 36, Tulsa, Oklahoma.

Ford, T.D., Pedley, H.M. (1996). A review of tufa and travertine deposits of the world. Earth-Science Reviews 41: 117-175.

Freytet, P., Verrecchia, E. P. (2002). Lacustrine and palustrine carbonate petrography: an overview, Journal of Paleolimnology 27: 221–237.

Greensmith, J. T. (1978). Petrography of the Sedimentary Rocks. 6th. edition. George Allen and UNWIN, London.

Guo, L., Riding, R. (1998). Hot spring travertine facies and sequence, Late Pleistocene, Rapolano Terme, Italy. Sedimentology 45: 163-180.

Hasan, M. R., Chakrabarti, R. (2009). Use of algae and aquatic macrophytes as feed in small-scale aquaculture: a review. FAO Fisheries and Aquaculture Technical Paper No.531 pp.

Ibrahim, K. M., Makhlouf, I. M., El Naqah, A. R., Al-Thawabteh, S. M. (2017). Geochemistry and Stable Isotopes of Travertine from Jordan Valley and Dead Sea Areas. Mineralogy 7(6): 82.

Kahle, C. F. (1977). Origin of subaerial Holocene calcareous crusts: role of algae, fungi and sparmicritization. Sedimentology 24: 413-435.

Kanellopoulos, C., Thomas, C., Xirokostas, N., Ariztegui, D. (2018). Banded Iron Travertines at the Ilia Hot Spring (Greece): An interplay of biotic and abiotic factors leading to a modern Banded Iron Formation analogue? Depositional Record 5: 109-130. https://doi.org/10.1002/dep2.55

Kitano, Y. (1963). Geochemistry of calcareous deposits found in hot springs. J. Earth Sciences 11: 68-100. Nagoya University.

Love, K. M., Chafetz, H. S. (1988). Diagenesis of laminated travertine crusts, Arbuckle Mountains, Oklahoma. J. Sedimentary Petrology 58: 441-445.

Love, K. M., Chafetz, H. S. (1990). Petrology of Quaternary travertine deposits, Arbuckle Mountains, Oklahoma. In: Hermann, J. S. and Hubbard Jr., D. A. (editors), Travertine-marl: Stream Deposits of Virginia. Virginia Division of Mineral Resources Publication 101, Charlottesville, Va. (Virginia Division of Mineral Resources).

Macintyre, I.G., Prufert-Bebout, L., Reid, R.P. (2000). The role of endolithic cyanobacteria in the formation of lithified laminae in Bahamas stromatolites. Sedimentology 47, 915–921.

Obeidat, O. (1992). Geochemistry, Minerology, and Petrography of Travertine of Deir Alla and Zerqa Ma'in Hot Springs. Unpublished M.Sc. Thesis, Yarmouk University. Irbid, Jordan.

Özkul, M., Varol, B., Alçiçek, C. (2002). Depositional environments and petrography of Denizli travertines. Bulletin of the Mineral Research and Exploration 125: 13-29.

Özkul, M., Gökgöz, A., Kele, S., Baykara, M. O., Shen, C.,

Chang,Y., Kaya, A., Hançer, M., Aratman, C., Akin, T., Örü, Z (2014). Sedimentological and geochemical characteristics of a fluvial travertine: A case from the eastern Mediterranean region. Sedimentology 61: 291-318.

Pache, M., Reitner, J., Arp, G. (2001). Geochemical evidence for the formation of a large Miocene "travertine" mound at a sublacustrince spring in a soda lake (Wallertein Casrtle Rock, Nördinger Ries, Germany). Facies 45: 311-330.

Pedley, H. M. (1994). Prokaryote-microphyte biofilms and tufas: a sedimentological perspective. Kaupia 4: 45-60.

Pentecost, A. (1990). Calcification processes in algae and cyanobacteria. p. 3-20. In R. Riding, éd., Calcareous algae and stromatolites. Springer-Verlag, Berlin: 569 p.

Pentecost, A. (2005). Travertine. 1st. edition. Springer, London.

Pola, M., Fabbri, P., Piccinini, L., Zampieri, D. (2013). A new hydrothermal conceptual and numerical of the Euganean Geothermal System – NE Italy. Bollettino della Società geologica italiana 24: 251–253.

Reolid, M., Rodríguez-Tovar, F.J., Nagy, J., Olóriz, F. (2008). Benthic foraminiferal morphogroups of mid to outer shelf environments of the Late Jurassic (Prebetic Zone, Southern Spain): Characterization of biofacies and environmental significance. Palaeogeography, Palaeoclimatology, Palaeoecology 261: 280-299.

Riding, R. (2000). Microbial carbonates: the geological record of calcified bacterial-algal mats and biofilms. Sedimentology: 47, 179-214.

Soulié-Märsche, I., García, A. (2015). Gyrogonites and oospores, complementary viewpoints to improve the study of the charophytes (Charales), Aquatic Botany 120, (A): 7-17. https://doi.org/10.1016/j.aquabot.2014.06.003

Suosaari, E. P., Reid, R. P., Oehlert, A. M., Playford, P. E., Steffensen, C. K., Andres, M. S., Suosaari, G.V., Milano, G.P., Eberli, G. P. (2019). Stromatolite provinces of hamelin pool: Physiographic controls on stromatolites and associated lithofacies. Journal of Sedimentary Research 89(3): 207–226. https://doi.org/10.2110/jsr.2019.8

Visscher, P.T., Reid, R.P., Bebout, B.M. (2000). Microscale observations of sulfate reduction: correlation of microbial activity with lithified micritic laminae in modern marine stromatolites. Geology 28: 919–922.